small methods
www.small-methods.com

Differentiating Between V- and G-Series Nerve Agent and Simulant Vapours Using Fluorescent Film Responses

Shengqiang Fan, Alex S. Loch, Kylie Vongsanga, Genevieve H. Dennison, Paul L. Burn, Ian R. Gentle, and Paul E. Shaw*

In-field rapid and reliable identification of nerve agents is critical for the protection of Defence and National Security personnel as well as communities. Fluorescence-based detectors can be portable and provide rapid detection of chemical threats. However, most current approaches cannot differentiate between dilute vapors of nerve agent classes and are susceptible to false positives due to the presence of common acids. Here a fluorescence-based method is shown for rapid differentiation between the V-series and phosphonofluoridate G-series nerve agents and avoids false positives due to common acids. Differentiation is achieved through harnessing two different mechanisms. Detection of the V-series is achieved using photoinduced hole transfer whereby the fluorescence of the sensing material is quenched in the presence of the V-series agent. The G-series is detected using a turn-on mechanism in which a silylated excited state intramolecular proton transfer sensing molecule is selectively deprotected by hydrogen fluoride, which is typically found as a contaminant and/or breakdown product in G-series agents such as sarin. The strategy provided discrimination between classes, as the sensor for the G-series agent class is insensitive to the V-series agent, and vice versa, and neither responded to common acids.

1. Introduction

The use of chemical warfare agents (CWAs), particularly nerve agents,[1] is a significant concern. Known nerve agents all contain a phosphorous-oxygen double bond and are generally defined by the nature of the leaving group attached to the phosphorous atom (Figure S1, Supporting Information). G-series nerve agents generally contain a phosphorous-fluorine bond, with the notable exception being tabun, which has a cyano leaving group. In contrast, the best-known V-series agent, VX, has alkoxy and alkylthio groups attached to the phosphorous atom. The nature of the hazard presented by the release of a nerve agent is dependent on its vapor pressure, toxicity, and environmental stability. For example, the median lethal vapor concentration (LC_{50}) of VX is four times lower than sarin (1.2 ppm), but sarin has a vapor pressure over 4000 times higher at 20 °C.[2,3] Additionally, as VX is much less reactive with water vapour than sarin, the former represents a much more persistent deposited hazard in the environment.[4] Thus, identifying which class of nerve agent is present is critical for personnel to make decisions about protection and hazard management protocols. Independent of the nerve agent structure, they all act as competitive inhibitors for acetylcholine, which is a neurotransmitter[1,5] and death often occurs by suffocation due to inability of the victim to control the muscles required for breathing. Current detection methods for nerve agent contamination may be affected by environmental interferents, and include enzyme-based colorimetric kits, which require the collection of samples (solids or liquids) from surfaces and generally take two to three minutes to show a color change,[6] and vapor detectors such as portable ion mobility spectrometers.[7] Fluorescence-based sensing is an attractive approach for the detection of chemical threats, with its feasibility demonstrated through deployment of lightweight portable devices capable of detecting explosive vapors using solid-state sensing films.[8–11] It is therefore not surprising that effort has been put into the development of fluorescent materials that can detect nerve agents. Fluorescent-based sensors can be lightweight, have low power consumption, provide rapid, sensitive, and in some cases selective detection of chemical threats.

S. Fan, A. S. Loch, P. L. Burn, I. R. Gentle, P. E. Shaw
Centre for Organic Photonics & Electronics (COPE)
School of Chemistry & Molecular Biosciences
University of Queensland
St. Lucia, QLD 4072, Australia
E-mail: p.burn2@uq.edu.au

K. Vongsanga, G. H. Dennison
CBRN Defence Branch
Sensors and Effectors Division, Defence Science and Technology Group
Fishermans Bend, VIC 3207, Australia

G. H. Dennison
Electro Optic Sensing and Electromagnetic Warfare
Sensors and Effectors Division, Defence Science and Technology Group
Edinburgh, SA 5111, Australia

The ORCID identification number(s) for the author(s) of this article can be found under https://doi.org/10.1002/smtd.202301048

DOI: 10.1002/smtd.202301048

Although the use of metal complex-based phosphorescent emitters and fluorescent chromophores capable of hydrogen bonding has been explored for the detection of nerve agents and simulants,[12–15] the majority of fluorescence-based sensing materials research has focused on chromophores containing nucleophilic components and, in particular, nitrogen-based nucleophiles.[16–19] The latter strategy aims to utilize the electrophilicity of the phosphorous atom of the nerve agent, where the nucleophilic nitrogen atom attacks the phosphorous electrophile, with the subsequent loss of a leaving group leading to modulation of the fluorescence properties of the sensing material. However, there are limitations with the nucleophilic substitution strategy, including the rate of the solid-state reactions (as thin film sensing is required for a portable detector), selectivity (as any difference in reactivity of the V- and G-series agents can be subtle),[14,20,21] and finally, amines are both nucleophiles and Lewis bases and hence the presence of common acids (e.g., hydrochloric acid and acetic acid) can elicit a similar response to G-series agents leading to false positives.[18,22] This latter point will be discussed in further detail later. It is important to note that to date, there are no fluorescent sensors reported that are able to rapidly detect and differentiate dilute vapors of V- and G-series agents.[18,22] Our approach to achieving detection and differentiation of dilute vapors of the V- and G-series nerve agent classes is built on an understanding of the chemical properties of the agents. It should be noted that due to the toxicity of nerve agents, most previously reported studies use simulants [e.g., di-*iso*-propyl fluorophosphate (DFP)[23] and 2-(di-*iso*-propylamino)ethyl ethyl methylphosphonate (VO)],[13] and that while the simulants are less toxic than the nerve agents they are still highly toxic. DFP is commonly used to simulate the reactivity of the phosphorous-fluorine (P-F) bond in the G-series phosphonofluoridate agents, while VO was developed to investigate supramolecular interactions of V-series agents. In addition to studies on the standard simulant we tested two exemplar sensing materials against nerve agents at the Defence Science and Technology Group, which is recognized by the Organisation for the Prohibition of Chemical Weapons (OPCW) as being allowed to conduct research with CWAs for protective purposes.

2. Results and Discussion

2.1. Sensing Mechanisms

2.1.1. G-Series Nerve Agents

G-series agents (Figure S1, Supporting Information), such as sarin, contain hydrogen fluoride as a side product of their synthesis as well as from hydrolysis of the P-F bond from atmospheric water.[4] Our strategy therefore focused on detecting the hydrogen fluoride that is always present in impure sarin samples. The simulant DFP is also not stable to hydrolysis, and if not protected from water will contain hydrogen fluoride.[24] In organic synthesis, fluoride reagents are used to cleave silyl protecting groups attached to alcohols. However, the use of a deprotection strategy is not sufficient in itself, as fluorescent chromophores that have unprotected or silylated hydroxyl groups can often have similar fluorescence spectra (Figure S2, Supporting Information). Hence, we have developed a sensing material capable of undergoing excited state intramolecular proton transfer (ESIPT)[25] in its deprotected form to provide a dramatic change in the fluorescent properties (**Figure 1**). For the sensing material (Sensor) in Figure 1, the silyl protected chromophore has emission peaks at 378 nm and 392 nm, while the ESIPT emission of the deprotected form (the Reporter, Figure 1) has a peak at 471 nm (Figure S3, Supporting Information). That is, the key innovation is that as the silyl group is removed by the hydrogen fluoride in sarin or the simulant (see Figure S4, Supporting Information), the intensity of the emission associated with the ESIPT reporter increases and a turn-on response is observed (Figure 1). Each subsequent exposure of the sensing material to the simulant vapor leads to an additional increase in the PL intensity (Figure S5, Supporting Information). However, a challenge with turn-on based detection is differentiation between a small increase in fluorescence caused by the detection event from the background fluorescence of the initial chromophore. This background fluorescence, no matter how weak, can reduce the sensitivity of the detector. We overcame this problem by designing the ESIPT Reporter emitter such that its absorption onset was red shifted relative to the silyl protected Sensor compound (Figure S3, Supporting Information) with a larger absorption coefficient at the excitation wavelength of 365 nm meaning that it more strongly absorbed the incident light. The difference in film emission of the sensor material and that of the reporter compound is evident in the photos in Figure 1 as is the increase in PL intensity measured upon exposure to DFP and sarin. It will be appreciated that the sensing of hydrogen fluoride is an irreversible process as the deprotection of the sensor material cannot be reversed.

2.1.2. V-Series Nerve Agents

The V-series nerve agents do not contain fluorine substituents (Figure S1, Supporting Information) and hence are typically not contaminated with hydrogen fluoride. As a consequence, they cannot deprotect the silyl protected hydroxyl group of the Sensor material to form the ESIPT Reporter compound. To detect the V-series agents we utilized the facts that they contain a tertiary amine group and that tertiary amines are known to undergo photoinduced hole transfer (PHT).[26] However, there are few reported organic semiconductor materials that are fluorescent in the solid state and have a sufficiently large ionization potential to induce PHT of tertiary amines. We have therefore developed a compound composed of a fluorenylbenzothiadiazole moiety and dicyanovinyl group that is capable of PHT with the amine moieties found in the V-series nerve agents (**Figure 2**). The sensing material is fluorescent in the solid-state, but in the presence of VX or the simulant VO, PHT occurs, and the fluorescence of the sensing material is quenched (Figure 2) – a turn-off mechanism. However, in this case, the process is reversible in that the intermolecular charge transfer state can decay non-radiatively to the ground state, and when the nerve agent exits the film, the fluorescence intensity recovers (Figure 2). An important point with regard to differentiating between the V- and G-series is that the silylated material designed to detect the G-series agents does not have a sufficiently large ionization potential to enable PHT to occur with the V-series vapors, which will be discussed in the next section.

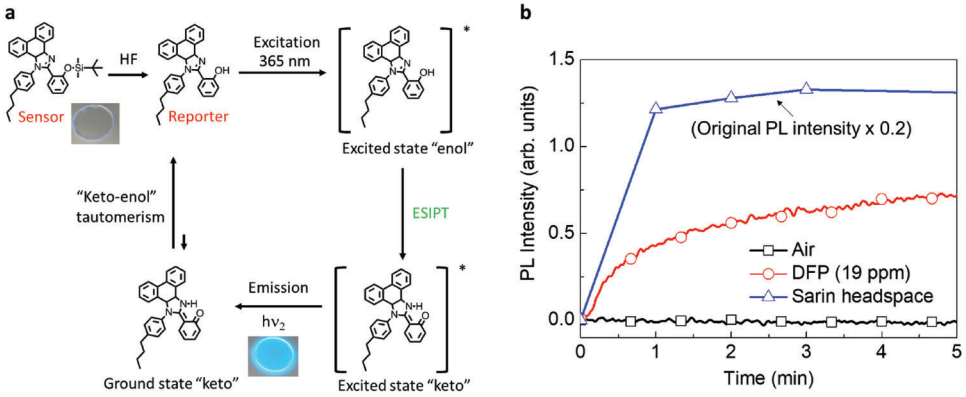

Figure 1. Mechanism for phosphonofluoridate G-series nerve agent and simulant detection. a) The hydrogen fluoride present in the nerve agent removes the silyl protecting group of the Sensor material to leave an ESIPT Reporter compound, which emits at a longer wavelength. b) The change in the PL intensity (excitation at 365 nm) from the sensing film in the presence of DFP (Method B – see Experimental Section) or sarin (Method A). No change in the PL intensity is observed when the Sensor material is exposed to air. The synthesis of the Sensor material is described in the Supplementary Information.

2.2. Acid Selectivity

Common acids such as hydrochloric and acetic acid are interferents for reported nucleophile-based luminescence sensors designed to detect G- and V-series agents and simulants.[18,22] In this work we explored the ability of the sensing materials to discriminate between the V- and G-series and demonstrate that common acids such as hydrochloric and acetic acid do not elicit a false positive response. Discrimination between the G- and V-series was achieved in several ways. First, the V-series sensor does not have functional groups capable of responding to the hydrogen fluoride found in the phosphonofluoridate G-series nerve agents and simulants. In addition, the ionization potential of the silylated G-series sensing material was engineered to be insufficiently deep for efficient PHT with the V-series agents and simulants, and finally, the G-series response is an irreversible PL turn-on mechanism while detection of the V-series is a reversible turn-off process. The contrasting responses of both sensing materials to the agents and simulants of each class are illustrated in **Figure 3**. It can be seen that the silylated material only responds to the hydrogen fluoride in sarin and DFP (PL turn-on), with no response to VX or VO. In contrast, the PL intensity of the V-series sensing material is quenched with VX and VO and there is no change in the presence of sarin or DFP. Thus, we have demonstrated that the vapors from V- and G-series agents can be differentiated from each other. We have also tested the response of the two sensing materials against hydrochloric and acetic acids with the results shown in Figure S7 (Supporting Information). As expected the PL of the V-series sensing material was not quenched by either acid. However, critically the silylated sensing material was not deprotected upon exposure to either acid and there was no PL turn-on. The lack of reactivity is due to both the relative bond strengths – the silicon-fluorine bond (565 kJ mol^{-1}) is stronger than the silicon-oxygen (452 kJ mol^{-1}) and silicon-chlorine (381 kJ mol^{-1}) bonds – and the steric encumbrance of the dimethyl-*t*-butylsilyl protecting group.

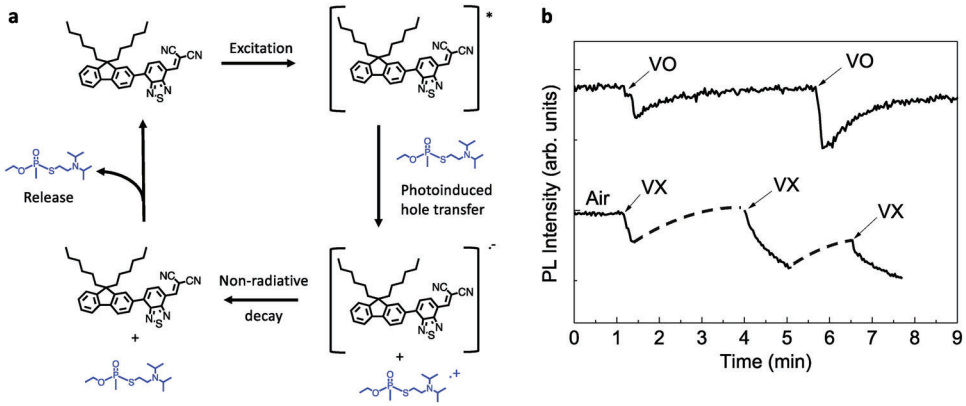

Figure 2. Mechanism and response for VX and VO detection. a) V-series detection – the sensor compound fluoresces in the absence of the agent/simulant. In the presence of the agent/simulant the fluorescence is quenched via PHT (VX is shown). The intramolecular charge transfer state then decays non-radiatively to the ground state and the fluorescence recovers. b) The PL intensity response against VO vapor (≈650 ppb) for two 5 s injections (0.5 mL, 1 mL – left to right) and VX headspace. The extrapolated recovery of the PL intensity of films exposed to VX is indicated by the dashed lines, with the data taken from Figure S6 (Supporting Information). The response of the sensing material in "Air" was measured using a separate film, which was used to normalize the PL intensity value. The synthesis of the sensing material is described in the Supplementary Information.

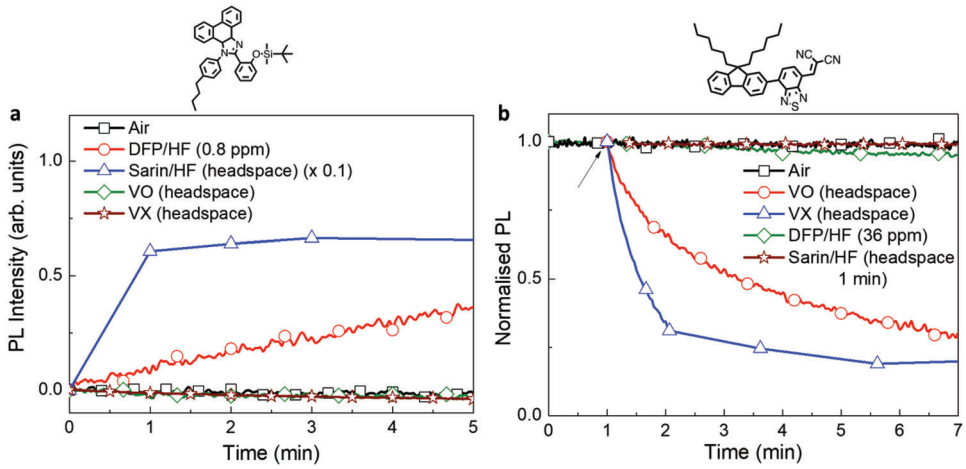

Figure 3. Responses of the sensing materials against sarin, DFP, VX, and VO. a) Response of the ESIPT-based sensor. b) Response of the sensor designed to undergo PHT. DFP purity was 99% (^{19}F NMR) with ≈1% HF. VO purity was 98%. Saturated VO vapor was generated using Method A while diluted DFP vapor was produced using Method B (see Figure S8 (Supporting Information) and Experimental Section).

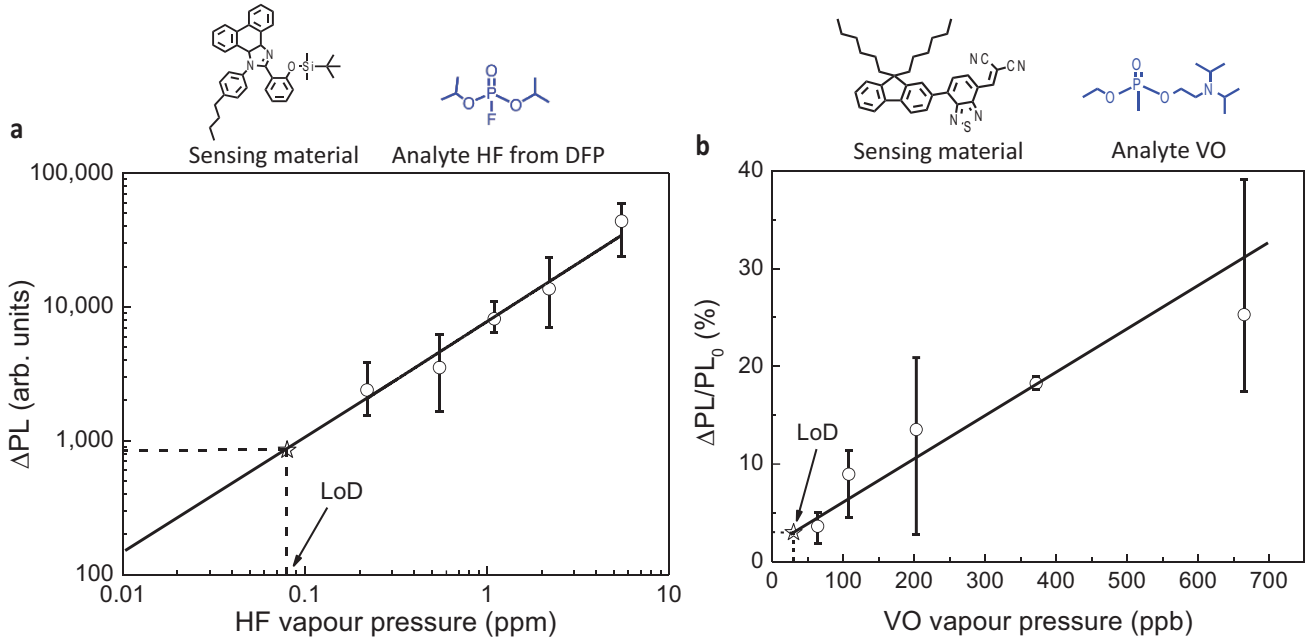

Figure 4. Limit of detection of the sensing materials. a) Method B (see Methods section) was used to produce the DFP vapor. The liquid DFP had a purity of 99% (≈1% HF) and for the LoD determination of each it was assumed that all the hydrogen fluoride was in the vapor phase. The ΔPL corresponds to the change in PL intensity after five minutes of exposure to DFP vapor. b) Method A was used to generate VO vapor with a pressure ranging from ≈100 to ≈650 ppb. The PL quenching ratio ($\Delta PL/PL_0$) was determined using the PL decrease after 5 min.

2.3. Sensitivity

The LC_{50} values of sarin and VX are 1.2 and 0.3 ppm, respectively.[3] It is important to note that the vapor pressures of VO and VX are similar.[27,28] We therefore investigated the limit of detection (LoD) for VO noting that in each case it was determined using three times the standard deviation (3σ) of the change in PL intensity in air. The percentage of PL quenching of the V-series sensing material was found to be proportional to the VO vapor pressure with the LoD determined to be ≈30 ppb (**Figure 4**), which is lower than the LC_{50} values of VX (80-160 ppb for a 5 min exposure, see Table S1, Supporting Information[3]). Our method for detecting sarin from the hydrogen fluoride present makes it difficult to determine the LoD of the agent itself as the amount of acid present is dependent on the purity of the agent. For example, the sarin that was used in the 1995 attack in Japan had a purity of only 25% and hence would be expected to contain hydrogen fluoride.[29] Therefore, to gain an idea of the LoD for sarin we used DFP that contained 1% of hydrogen fluoride, with the hydrogen fluoride concentration determined using fluorine

NMR spectroscopy. We found that the increase in the PL signal was proportional to the amount of hydrogen fluoride present (Figure 4a) and from this we determined the effective LoD of DFP containing the 1% of hydrogen fluoride to be ≈0.3 ppm. Sarin is four times more volatile than DFP,[4] and assuming the same concentration of hydrogen fluoride being present would suggest that this method can effectively detect sarin at a concentration of ≈1.2 ppm, which is lower than the LC_{50} value (1.6-3.2 ppm for 5 min exposure, see Table S1, Supporting Information).[3]

3. Conclusion

Drawing all the results together it can be seen that our approach is a step change in fluorescence-based vapor detection and differentiation of G- and V-series nerve agents and their simulants. By moving away from the typical approach of using sensing materials containing nucleophilic groups we have been able to avoid false positive responses associated with common acids and difficulties in identifying which nerve agent class is present. Recognizing that sarin typically contains hydrogen fluoride we have developed a sensing material that selectively reacts with the acid to release an ESIPT chromophore. The use of the ESIPT chromophore avoids issues relating to background fluorescence and detection is via a turn-on mechanism. Importantly, the ionization potential of the G-series sensing material is not sufficient to have its PL quenched by VO or VX. In contrast, the V-series sensing material has its PL reversibly quenched by VO and VX with DFP, hydrogen fluoride, and sarin having no effect. That is, we have demonstrated the first example of a fluorescence-based vapor sensing approach for the differentiation of the G- and V-series nerve agents that is not susceptible to acid interferents. Finally, in addition to class differentiation, we have also demonstrated that this approach has the sensitivity to potentially detect below the LC_{50} of the two nerve agents.

4. Experimental Section

Film Preparation: Films of 20–30 nm thickness were spin-coated onto fused silica substrates. 2-[4-({*Tert*-butyldimethylsilyl}oxy)phenyl]−1-[(4-butylphenyl]−1*H*-phenanthro[9,10-*d*]imidazole and 2-[(7-{9,9-i-*n*-hexyl-9*H*-fluoren-2-yl}benzo[*c*][1,2,5]thiadiazol-4-yl)methylene]malononitrile were dissolved in toluene and chloroform, respectively, at a concentration of 10 mg mL^{-1} and then spin-coated using a Specialty Coating Systems, G3P-8 at 2000 and 5000 r.p.m for the former and latter compound, respectively, with a 60 s dwell and 1 s ramp.

Sensing: The work on CWAs and their simulants was conducted by trained professionals in appropriate facilities for protective purposes. GB and VX are Schedule 1 chemicals under the Chemical Weapons Convention, and their extreme toxicity and potency arising from acetylcholinesterase inhibition leads to incapacitation and death at low concentrations. Their synthesis and experimentation are regulated under national laws and with international oversight from the Organisation for the Prohibition of Chemical Weapons (OPCW). Unless noted (see Figure S8, Supporting Information), two methods were used for the generation of the analyte vapor and measurement of the changes in the PL. **Method A**: the simulants (2 µL for DFP or VO) or actual nerve agents (a pipette drop for sarin and VX) were added onto a Teflon lid, which was then placed at the bottom of the optical chamber. The optical chamber for the DFP measurements was made from PTFE, with the temperature kept at 20°C. The vapor pressure of DFP at 20°C is 770 ppm.[30] The chamber for the VO tests was made from titanium and the vapor pressure was controlled by varying the temperature of the chamber between 1 and 20 °C using a brine/ice bath. The VO vapor pressure was estimated based on the calculated value being close to the VX vapor pressure at the same temperatures.[27,28] **Method B**: Analyte (2 µL for DFP or VO and 20 µL for hydrochloric acid or acetic acid) was added to a plastic syringe (10 mL) and kept for 30 min to allow the analyte to evaporate at 20 °C. The vapor was then injected into a nitrogen flow (200 mL min^{-1}) using a syringe pump at a flow rate of 0–20 mL min^{-1} and the mixed gas was introduced into the optical chamber for the sensing measurement. The waste vapor stream was passed through a scrubbing solution (20 wt.% sodium hydroxide in water) to neutralise the excess acid and/or break down the excess simulant. The vapor pressure was estimated by the dilution factor. The hydrogen chloride vapor pressure was controlled by the headspace of 32% or 16% hydrochloric acid solution[31] and dilution, while the acetic acid vapor pressure was controlled by dilution. The sensing film samples on fused silica substrates were mounted in the optical chamber which was connected to an LED light source (365 nm, OceanOptics) for excitation of the films and a spectrometer (Flame, OceanOptics) for subsequent detection of the film PL. The geometry was such that the excitation and detection paths were at right angles. Exemplars of the changes in the fluorescence are shown in Figure S9 (Supporting Information). Film PL spectra before and after exposure to the analyte and PL kinetics were recorded with OceanView software (OceanOptics). The PL intensity in the kinetics measurements represents an integrated value over the wavelength range of 420–600 nm for the G-series detection and 500–800 nm for the V-series detection.

Supporting Information

Supporting Information is available from the Wiley Online Library or from the author.

Acknowledgements

P.L.B. is a UQ Laureate Fellow. This research was supported by funding from the Australian Research Council under the Discovery Program (DP170102072).

Open access publishing facilitated by The University of Queensland, as part of the Wiley - The University of Queensland agreement via the Council of Australian University Librarians.

Conflict of Interest

The authors declare no conflict of interest.

Data Availability Statement

The data that support the findings of this study are available from the corresponding author upon reasonable request.

Keywords

fluorescence, G-series nerve agents, thin films, vapour detection, V-series nerve agents

Received: August 17, 2023
Revised: September 21, 2023
Published online:

[1] S. Costanzi, J.-H. Machado, M. Mitchell, *ACS Chem. Neurosci.* **2018**, *9*, 873.
[2] Y. J. Jang, K. Kim, O. G. Tsay, D. A. Atwood, D. G. Churchill, *Chem. Rev.* **2015**, *115*, PR1.

[3] S. W. Wiener, R. S. Hoffman, *J. Intensive Care Med.* **2004**, *19*, 22.
[4] D. H. Rosenblatt, M. J. Small, T. A. Kimmell, A. W. Anderson, Background chemistry for chemical warfare agents and decontamination processes in support of delisting waste streams at the U.S. Army Dugway Proving Ground, Utah. OSTI, USA **1996**. pp. 8–35.
[5] R. T. Delfino, T. S. Ribeiro, J. D. Figueroa-Villar, *J. Braz. Chem. Soc.* **2009**, *20*, 407.
[6] F. N. Diauudin, J. I. A. Rashid, V. F. Knight, W. M.d Z. Wan Yunus, K. K. Ong, N. A. M. Kasim, N. Abdul Halim, S. A. M. Noor, *Sens. Bio-Sens. Res.* **2019**, *26*, 100305.
[7] M. A. Mäkinen, O. A. Anttalainen, M. E. T. Sillanpää, *Anal. Chem.* **2010**, *82*, 9594.
[8] P. E. Shaw, P. L. Burn, *Phys. Chem. Chem. Phys.* **2017**, *19*, 29714.
[9] X. Sun, Y. Wang, Y.u Lei, *Chem. Soc. Rev.* **2015**, *44*, 8019.
[10] Y. Salinas, R. Martínez-MáñEz, M. D. Marcos, F. Sancenón, A. M. Costero, M. Parra, S. Gil, *Chem. Soc. Rev.* **2012**, *41*, 1261.
[11] S. W. Thomas, G. D. Joly, T. M. Swager, *Chem. Rev.* **2007**, *107*, 1339.
[12] D. Knapton, M. Burnworth, S. J. Rowan, C. Weder, *Angew. Chem., Int. Ed.* **2006**, *45*, 5825.
[13] G. H. Dennison, C. G. Bochet, C. Curty, J. Ducry, D. J. Nielsen, M. R. Sambrook, A. Zaugg, M. R. Johnston, *Eur. J. Inorg. Chem.* **2016**, *2016*, 1348.
[14] G. H. Dennison, C. Curty, A. J. Metherell, E. Micich, A. Zaugg, M. D. Ward, *RSC Adv.* **2019**, *9*, 7615.
[15] E. Butera, A. Zammataro, A. Pappalardo, G. Trusso Sfrazzetto, *ChemPlusChem* **2021**, *86*, 681.
[16] B. Zhu, R. Sheng, T. Chen, J. Rodrigues, Q.-H. Song, X. Hu, L. Zeng, *Coord. Chem. Rev.* **2022**, *463*, 214527.
[17] W.-Q.i Meng, A. C. Sedgwick, N. Kwon, M. Sun, K. Xiao, X.-P. He, E. V. Anslyn, T. D. James, J. Yoon, *Chem. Soc. Rev.* **2023**, *52*, 601.
[18] S. Fan, G. Zhang, G. H. Dennison, N. Fitzgerald, P. L. Burn, I. R. Gentle, P. E. Shaw, *Adv. Mater.* **2019**, *32*, 1905785.
[19] L. Chen, D.i Wu, J. Yoon, *ACS Sens.* **2018**, *3*, 27.
[20] X. Sun, A. A. Boulgakov, L. N. Smith, P. Metola, E. M. Marcotte, E. V. Anslyn, *ACS Cent. Sci.* **2018**, *4*, 854.
[21] O. Redy Keisar, A. Pevzner, A. Baheti, A. Vigalok, N. Ashkenazi, *Chem. Commun.* **2020**, *56*, 15040.
[22] S. Fan, G. H. Dennison, N. Fitzgerald, P. L. Burn, I. R. Gentle, P. E. Shaw, *Commun. Chem.* **2021**, *4*, 45.
[23] S. El Sayed, L. Pascual, A. Agostini, R. Martínez-MáñEz, F. Sancenón, A. M. Costero, M. Parra, S. Gil, *ChemistryOpen* **2014**, *3*, 142.
[24] D. R. Heiss, D. W. Zehnder II, D. A. Jett, G. E. Platoff Jr., D. T. Yeung, B. N. Brewer, *J. Chem.* **2016**, 3190891.
[25] A. C. Sedgwick, L. Wu, H.-H. Han, S. D. Bull, X.-P. He, T. D. James, J. L. Sessler, B. Z. Tang, H.e Tian, J. Yoon, *Chem. Soc. Rev.* **2018**, *47*, 8842.
[26] Y. Pellegrin, F. Odobel, *C. R. Chim.* **2017**, *20*, 283.
[27] J. H. Buchanan, L. C. Buettner, A. B. Butrow, D. E. Tevault, Vapor pressure of VX **1999**, https://apps.dtic.mil/sti/pdfs/ADA371297.pdf (accessed: January **2023**).
[28] SciFinder; Chemical Abstracts Service: Columbus, OH; Predicted properties of CAS Registry Number 71840-26-1 using Advanced Chemistry Development (ACD/Labs) Software V11.02 (© 1994–2023 ACD/Labs), https://scifinder.cas.org (accessed: January **2023**).
[29] A. T. Tu, *J. Mass Spectrom. Soc. Jpn.* **1996**, *44*, 293.
[30] S. Budavari, *The Merck index: an encyclopedia of chemical, drugs and biologicals*, 12th ed. Merck & Co., Whitehouse Station, NJ, USA **1996**, p. 883.
[31] D. Friend, B. Poling, G. Thomson, T. Daubert, E. Buck, *Physical and chemical data, Section 2*, McGraw Hill, NY, USA **2007**, p. 76.

